

See discussions, stats, and author profiles for this publication at: <http://www.researchgate.net/publication/278849501>

Numerical Simulation of Skewed Slot Effect on Local Scour Reduction

ARTICLE · JANUARY 2011

DOWNLOADS

5

VIEWS

8

4 AUTHORS, INCLUDING:



[Amir A. Dehghani](#)

Gorgan University of Agricultural Sciences ...

27 PUBLICATIONS 75 CITATIONS

[SEE PROFILE](#)

Numerical Simulation of Skewed Slot Effect on Local Scour Reduction

Taymaz Esmaili^{1*}, Amir Ahmad Dehghani², Mohammad Reza Pirestani³, Tetsuya Sumi⁴

1. Department of Civil Engineering, Aq Qala Center, Islamic Azad University, Aq Qala, Iran

2. Assistant Professor., Department of Water Engineering, Gorgan University of Agricultural Sciences & Natural Resources, Gorgan, Iran

3. Assistant Professor., Department of Civil Engineering, Islamic Azad University-South Tehran Branch, Tehran, Iran

4. Professor, Disaster Prevention Research Institute, Kyoto University, Uji- Kyoto 611-0011, Japan

Received: 11 Jun. 2011 ; Accepted: 27 Aug. 2011

ABSTRACT

Local scouring around bridge piers is a natural phenomenon caused by the erosive process of flowing stream on alluvial beds. The 3D flow field around bridge piers interacting with the bed materials increases complexity of local scour process. The local scour depth develops in accelerated flows and if it is not predicted correctly, the bottom level of local scour hole will exceed the original level of pier foundation. In this case the failure of bridge will occur. Using different methods of local scour countermeasure for reducing the magnitude of local scouring depth and retrofitting costs would be economically efficient. As a local scour countermeasure method, applying slots in the piers could reduce the local scour depth around circular piers. Since in natural streams the piers are skewed to flow in most cases, it is more feasible to evaluate the skew slots effects on scour reduction. The present study focuses on numerical simulation of maximum depth of scour due to the installing of slots in various angles of flow attacks by employing a 3D numerical model (SSIIM program). The results show the ability of SSIIM for modeling the local scouring around bridge piers with slots.

Keywords

Local scouring; Numerical model; Bridge pier; 3D numerical model; SSIIM program

1. Introduction

Due to the diverse economic and social costs that can be imposed by bridge failure the evaluation of the maximum local scour depth around bridge piers is an important topic in river engineering (Esmaili 2009). Local scouring around bridge piers can be a severe problem, especially when a high flow occurs in the river. When this undesirable event occurs, a scour hole appears around bridge piers. The local scour depth develops in high flows and if it is not predicted correctly the bottom level

of local scour hole will exceed the original level of the pier foundation. In this case the safety and stability of the bridge will be in danger. Bridge collapse during a flood raises many direct and indirect economic and social costs (Dehghani, et al. 2009). Streambed scour is the leading cause of bridge failure in the United States (Murillo 1987). The costs associated with restoring the damaged structures are substantial, but the indirect costs associated with the disruption of traffic are even more than four times the direct costs (Roheds and Trent 1993). The three-dimensional flow field around

* Corresponding Author Email: (taymaz.esmaili@gmail.com)

a pier is extremely complex due to the separation and generation of multiple vortices. The complexity of the flow field is further magnified due to the dynamic interaction between the flow and move-able boundary during the development of a scour hole (Raudkivi and Ettema 1985). Accurate prediction of scour pattern around bridge piers strongly depends on resolving the flow structure and the mechanism of sediment movement in and out of the scour hole (Mendoza-Cabrera 1993).

Many studies have been carried out to develop the relationships for predicting the maximum scour depth at bridge piers under clear-water scour condition and these relations have been used extensively for designing purposes (Dehghani et al. 2009). Implementation of bridges' pier foundation in a deeper depth than the maximum potential local scour hole was accepted as a conservative scour countermeasure in most of practical cases; although that would require expensive and deep piers in streambeds. Consequently, there is an interest in finding reliable ways to reduce scour depth and, thereby, requisite pier embedment depth. Furthermore, prior studies by the researchers regarding local scouring around bridge piers showed that geometric parameters of the pier is one of the most effective factors on the maximum local scour depth.

Efforts have been made to reduce scour by providing an array of piles in front of the pier (Chabert and Engeldinger 1956), a circular collar around the pier, (Thomas 1967, Tanaka and Yano 1967 and Ettema 1980), submerged vanes (Odgaard and Wang 1987), a delta-wing-like fin in front of the pier (Gupta and Gangadharaiyah 1992), combined methods (Garg, et al. 2008 and Moncada et al. 2009) a slot through the pier (Chew 1992), (Grimaldi et al. 2009) and (Tafarojnoruz et al. 2010).

Local scour around a solid pier results from the downflow at the upstream face of the pier and the horseshoe vortex at the base

of the pier. Hence, one way of reducing scour is to weaken and possibly prevent the formation of the downflow and horseshoe vortex. Depending on its location, a slot may deflect the downflow away from the bed by accelerating the bottom boundary layer flow through itself as a horizontal jet, and by breaking up the horseshoe vortex when the slot is placed near the bed. When placed near the water surface, a slot effectively reduces the downflow and horseshoe vortex. If ds_s is the depth of scour at a pier with a slot and ds_p is that for a pier without a slot, under the same flow conditions, Vittal et al. (1994), in their study of scour at a pier group, which is akin to a multislot, found that when ds_s/ds_p is plotted versus Y_L/Y_0 the value will be unique (Kumar et al. 1999).

Nowadays, numerical models are extensively used in simulating different problems in hydraulic science and one of these numerical models is SSIIM. This program was developed for using in river, environmental, hydraulic and sedimentation engineering. SSIIM is an abbreviation for sediment simulation in water intakes with multiblock options. This 3D CFD model was based on the finite volume method solving the Navier-Stokes equations using the various turbulence models (Olsen 1999).

In this study, the effect of slot on reduction of local scour depth reduction around a circular pier, by different lengths has been numerically simulated. Then the slots by different orientation to the flow have been simulated by SSIIM model and their potential to reduction of the maximum local scour depth around circular pier has been assessed.

2. The Numerical Model

SSIIM model was developed based on another Computational Fluid Dynamics model called SSII that was first introduced by N.R.B.

Olsen in 1990-91. SSII is an abbreviation for sediment simulations in intakes and it had the ability to apply 3D solution of convection-diffusion equation for sediment calculations. The main motivation for making SSII was the difficulty to simulate fine sediments in physical models. However, SSII model suffered from using a structured grid that made it possible just to have one block for an out blocked region while, in practical cases a multi-block model with general out blocking possibilities will be needed. Therefore, the capability of multi-block modelling was added to SSII and due to remarkable changes in the model, the new established model called SSIIM.

2.1. Tree-dimensional flow model

The SSIIM program solves the Navier-Stokes equations with the $k-\varepsilon$ model on a three dimensional general non-orthogonal coordinates. These equations are discretized with a control volume approach. The SIMPLE or SIMPLEC methods can be used for solving the pressure-Poisson equation. An implicit solver is used, producing the velocity field in the computational domain. The velocities are used when solving the convection-diffusion equations for different sediment size (Olsen 2007).

The Navier-Stokes equations for non-compressible and constant density flow can be modeled as:

$$\frac{\partial u_i}{\partial x_i} = 0 \quad (1)$$

$$\frac{\partial u_i}{\partial t} + u_j \frac{\partial u_i}{\partial x_j} = \frac{1}{\rho} \frac{\partial}{\partial x_j} \left(-P \delta_{ij} - \rho \overline{u'_i u'_j} \right) \quad (2)$$

The first term on the left side of the eq. [2] is the transient term. The next term is the convective term. The first term on the right-hand side is the pressure term and the second term on the right side of the equation is the Reynolds stress term. In order to evaluate this term, a turbulence model is required. SSIIM program can use different turbulence models, such as the standard $k-\varepsilon$ model or the $k-\omega$

model by Wilcox (2000). However, the default turbulence model is the standard $k-\varepsilon$ model.

The free surface is modeled as a fixed-lid, with zero gradients for all variables. The locations of the fixed lid and its movement are as a function of time, which can be computed by different algorithms. The 1D backwater computation is the default algorithm and it is invoked automatically. Pressure and Bernoulli algorithm can be used for both steady and unsteady computations. The algorithm is based on the computed pressure field. It uses the Bernoulli equation along the water surface to compute the water surface location based on one fixed point that does not move. The algorithm is fairly stable, so that it can also be used in connection with computation of sediment transport and bed changes (Olsen 2007).

For the wall boundary treatment, it is assumed that the velocity profile follows a certain empirical function called a wall law. It is a semi-analytical function to model the turbulence near the wall in the boundary layer and consequently the CFD model will not need to resolve the turbulence of flow in boundary layer. As a result, it would not to havenecessary too many grid points near the wall:

$$\frac{U}{u_x} = \frac{1}{\kappa} \ln \left(\frac{30y}{k_s} \right) \quad (3)$$

where the shear velocity is denoted u_x , κ is a constant equal to 0.4, y is the distance to the wall and k_s is the roughness equivalent to a diameter of particles on the bed.

2.2. Morphological model

The sediment transport process in rivers is described by the following equation, Exner's equation, which is the sediment continuity equation integrated over the water depth:

$$(1-\lambda) \frac{\partial z_b}{\partial t} + \frac{\partial q_{tx}}{\partial x} + \frac{\partial q_{ty}}{\partial y} = 0 \quad (4)$$

where z_b is the bed elevation, λ is the porosity of bed material, and q_{tx} and q_{ty} are components of total-load sediment transport in x- and y-directions, respectively.

In this 3D CFD program, the suspended load can be calculated with the convection-diffusion equation for the sediment concentration, which is expressed as follows:

$$\frac{\partial c}{\partial t} + u_j \frac{\partial c}{\partial x_j} + w \frac{\partial c}{\partial z} = \frac{\partial}{\partial x_j} \left(\Gamma_T \frac{\partial c}{\partial x_j} \right) \quad (5)$$

where w is the fall velocity of sediment particles and Γ_T is the diffusion coefficient and can be expressed in the following way:

$$\Gamma_T = \frac{\nu_T}{Sc} \quad (6)$$

where Sc is the Schmidt number representing the ratio of diffusion coefficient to eddy viscosity coefficient ν_t and set to 1.0 as default.

For calculating the suspended load in eq. [4], eq. [5] is solved incorporated with the formula by van Rijn (1987) for computing the equilibrium sediment concentration close to the bed as the bed boundary. In order to solve eq. [4] and eq. [5] conditions of z and C should be given at inflow and outflow boundaries. For the inlet boundary, due to the clear water scour conditions, $z=C=0$ can be given and for the outlet boundary, far away from the pier, $\frac{\partial C}{\partial x} = \frac{\partial z}{\partial x} = 0$ can be given due to the uniform flow.

The concentration formula has the following expression:

$$C_{bed} = 0.015 \frac{d^{0.3}}{a} \frac{\left[\frac{\tau - \tau_c}{\tau_c} \right]^{1.5}}{\left[\frac{(\rho_s - \rho_w)g}{\rho_w \nu^2} \right]^{0.1}} \quad (7)$$

where, C_{bed} is the sediment concentration, d is the sediment particle diameter, a is a reference level set equal to the roughness height, τ is the bed shear stress, τ_c is the critical bed shear stress for movement of

sediment particles according to Shield's curve, ρ_w and ρ_s are the density of water and sediment, ν is the viscosity of the water and g is the acceleration of gravity.

Once eq. [5] is solved, the suspended load can be calculated as follows:

$$q_{s,i} = \int_a^{z_f} u_i c \, dz \quad (8)$$

where $q_{s,i}$ ($i=1,2$) are components of suspended-load sediment transport in x- and y-directions, respectively.

For calculating the bed load in eq. [4], the following relation proposed by van Rijn's formula (1987) is used:

$$\frac{q_b}{D_{50}^{1.5} \sqrt{\frac{(\rho_s - \rho_w)g}{\rho_w}}} = 0.053 \frac{\left[\frac{\tau - \tau_c}{\tau_c} \right]^{1.5}}{D_{50}^{0.3} \left[\frac{(\rho_s - \rho_w)g}{\rho_w \nu^2} \right]^{0.1}} \quad (9)$$

where D_{50} is the mean size of sediment. Then, the components of bed-load sediment transport in x- and y-directions can be calculated as follows:

$$q_{bx} = q_b \cos(\alpha_b); \quad q_{by} = q_b \sin(\alpha_b) \quad (10)$$

where α_b is the direction of bed-load sediment transport.

3. Model properties and study case

Experimental results of Mia and Nago (2003) were used for calibration and validation of model.

Their experimental studies carried out in a flume 1600 cm long, 60 cm wide, and 40 cm deep, located in the Hydraulics Laboratory of Okayama University, Japan. Water was conveyed to the flume from an elevated tank by a pipe through an approach channel in which the discharge was measured by means of a sharp-crested weir.

The flow rate in the flume was adjusted using a valve. The water depth was adjusted with a tailgate. The head over the sharp crested weir and the water surface were

measured using a point gauge, sensitive to a variation of 0.1 mm. A mobile bed zone 100 cm long, 60 cm wide, and 57 cm deep was prepared at a distance 800 cm downstream of the flume beginning, and was filled with sediment of a median particle size $d_{50}=1.28$ mm and geometric standard deviation $\sigma_g=1.29$. A vertical circular pier of diameter $D=6$ cm was placed in the center of the mobile zone. The mobile bed was leveled before starting a test. The experiments were stopped at a stage when there was less than 1 mm scour by 1 h or no scour at all (Mia and Nago 2003). In their experimental study, temporal variation of scour depth under steady flows was measured and a method for calculating time variation of scour depth was proposed. Cross section and plan view of the flume has been illustrated in Fig. 1.

4. Numerical Simulations

4.1. Domain description and model calibration

Making an appropriate grid is a very important process in the preparation of input data for SSIIM program. The size and alignment of the cells will strongly influence the accuracy, the convergence and the computational time (Olsen 2007). For getting more precise results, it is better to refine the mesh around bridge piers (Dehghani, et al. 2009).

A preprocessing code was used for dividing flow field area into regions of different sizes. In this study, the length of channel is divided by eight sections and in each section the various cell sizes were used. The distribution of mesh in upstream half of the channel has been presented in Fig. 2. In the first region, in x- and y-directions, the size of cells is $2.5 \text{ cm} \times 0.5 \text{ cm}$, in the second region cells are $2 \text{ cm} \times 0.5 \text{ cm}$ and in the third region size is $1 \text{ cm} \times 0.5 \text{ cm}$. The central part of the flume is 1 m long and the size of cells is $0.5 \text{ cm} \times 0.5 \text{ cm}$. Due to the

vertical grid distribution, the total number of cells in the computational domain is 1128000.

For the inflow boundary condition, the velocity distribution was specified while the gradient of pressure is given zero. At the outflow boundary, the vertical gradient of velocity is zero and the hydrostatic pressure distribution is specified according to the water depth. For the solid boundary, wall laws introduced by Schlichting (1979) were used for the side walls and the bed. Moreover, the bed roughness can be given as a user input and it is a function of the experimental sediment size.

Moreover, in order to model verification another numerical run was conducted by the boundary condition of discharge equal to $0.04 \text{ m}^3/\text{s}$ and water level of 20 cm. In this case, computed equilibrium scour depth was 77.5 mm after 140 minutes, while experimental results showed the scour depth 78 mm. Fig. 3 illustrates the scour hole shape at the end of steady flow condition for calibration and verification stages.

The first step in running the numerical code is model calibration. In this study, by employing the experimental data of Mia and Nago (2003) in which, boundary condition of discharge and water level was $0.05 \text{ m}^3/\text{s}$ and 23.5 cm respectively, model was calibrated. When the model calibrated, the equilibrium local scour depth obtained 87.5 mm after 270 minutes whereas, the experimental data shows 89 mm at the end of corresponding time.

4.2. Simulation results and discussion

In order to numerically investigate the effect of slot without orientation on local scour reduction, different lengths of slots were employed. Kummur et al. (1999) concluded that the ratio of ds_s/ds_p is only a function of the dimensionless geometric parameters related to the slot, so the results of

their study employed on experimental runs of Mia and Nago (2003). In the selected experimental run, pier diameter was 6 cm and the boundary condition of discharge and water level were $0.04 \text{ m}^3/\text{s}$ and 20 cm respectively. The applied width of slot in the numerical simulation was half of the pier diameter that was equal to 3 cm. In order to compare the results of numerical model to experimental data, a dimensionless graph which was demonstrated in the study of Kummer et al. (1999), was employed. The mentioned graph had been obtained based on study of Chiew (1992) and the modification of Vittal et al. (1994). Fig.4 illustrates the geometry of slotted pier that was modelled in numerical simulations and effect of different length of

slot respect to water surface in the reduction of local scouring depth.

As can be clearly observed, when the length of slot increases and places near the bed, local scour depth starts to decrease. This is due to this fact that when slot length increases through the pier, vortices that have the major role in local scouring become weak. Fig. 4 also reveals that, numerical results have a good agreement with those gained through experimental runs. Although slot without orientation could reduce the magnitude of local scour depth as a local scour countermeasure, it is more feasible to evaluate the skewed slots' effects on the reduction of scour hole in natural streams where the position of piers are skewed to flow in most cases.

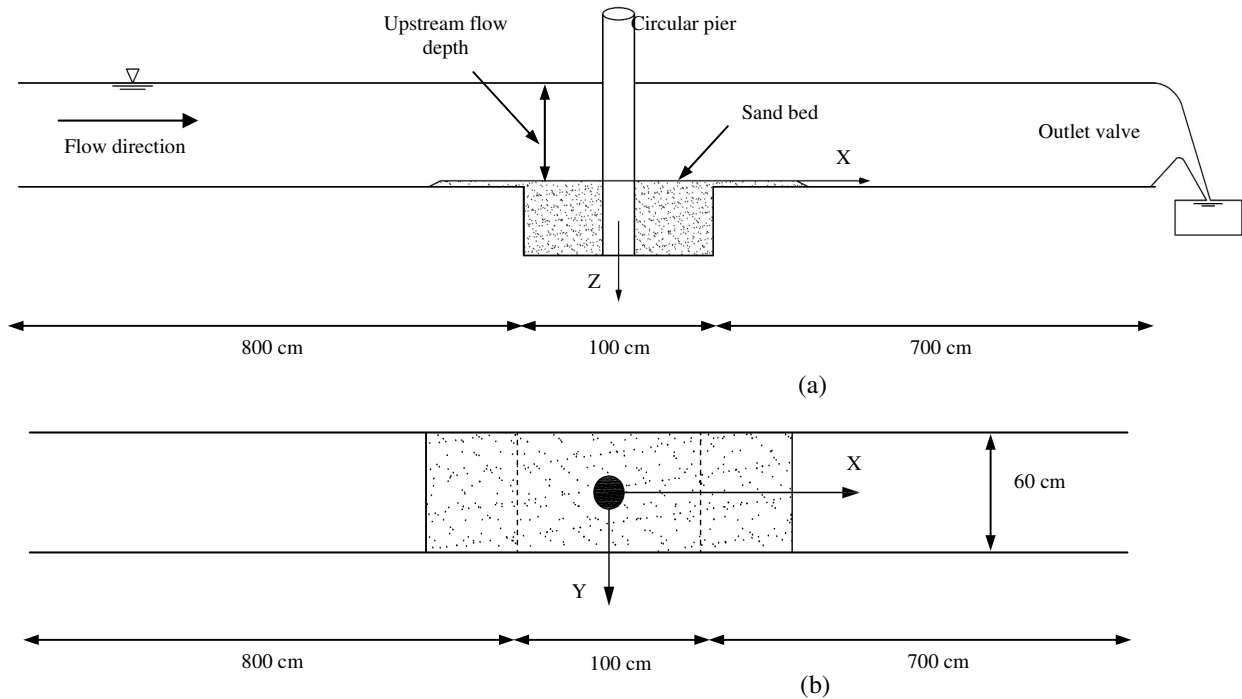


Fig. 1. Geometric properties of the flume in which experiments were done by Mia & Nago (2003); (a) longitudinal section, (b) plan view (not scaled).

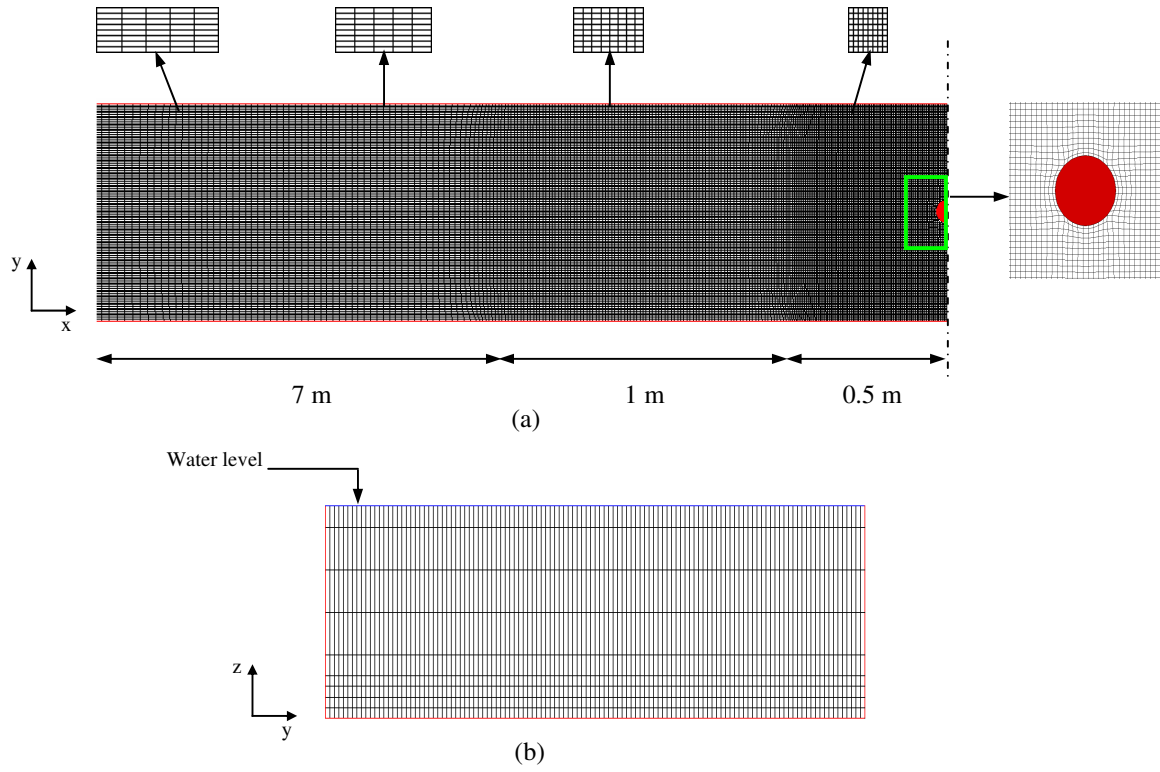


Fig. 2.(a) Plan view of computational domain used for numerical modeling (not scaled) and (b) Vertical grid distribution.

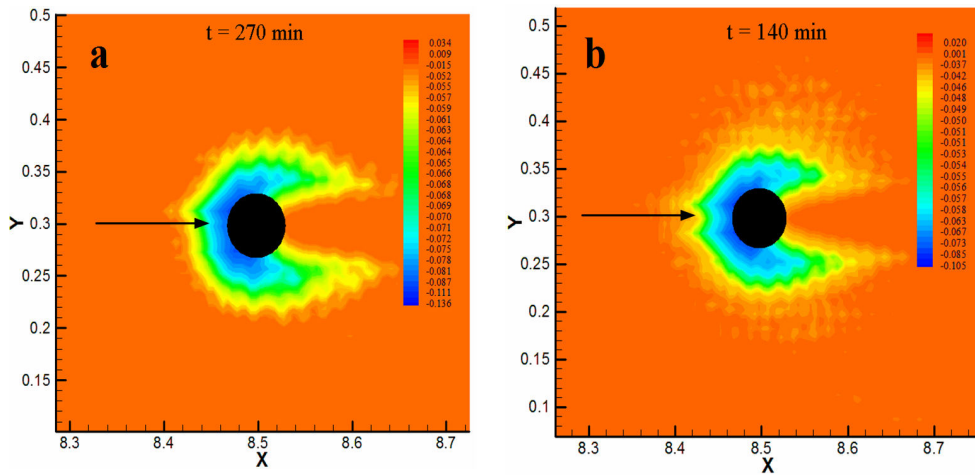


Fig. 3. (a) Bed changes in the vicinity of circular pier at the end of calibration and (b) verification stage

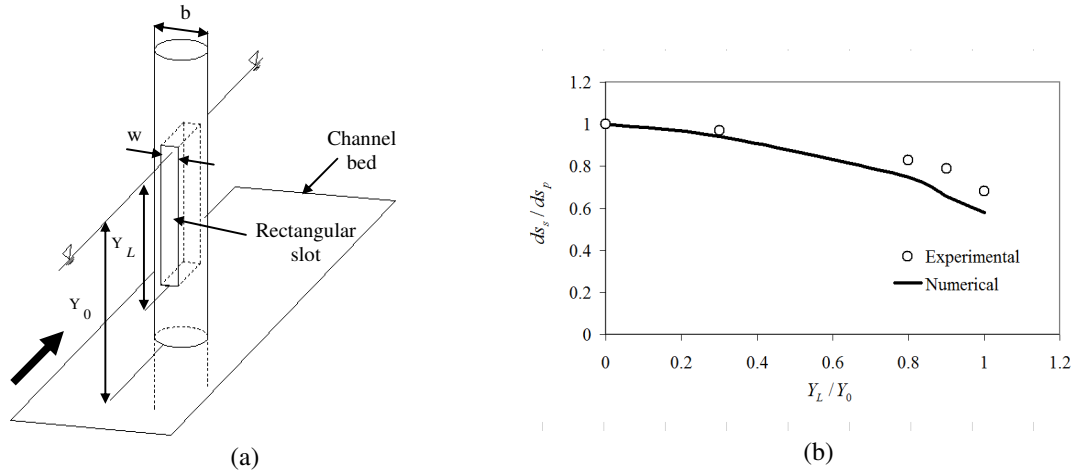


Fig. 4. (a) Geometric properties of slotted pier which was used in the study and (b) Variation of local scouring depth versus non-oriented slot length when the slot width is half of the pier diameter

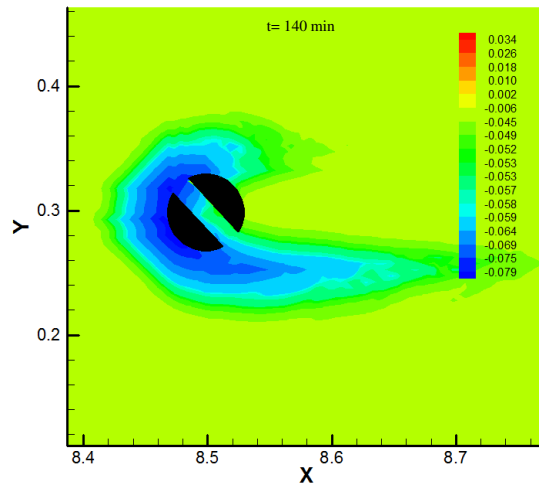


Fig. 5. Bed changes around pier with 45 degrees skewed slot at the end of recalibration stage

In regard to sensitivity of flow field and vortices pattern around skewed slots, model was recalibrated for the experiment of Mia & Nago (2003) in which the boundary condition of discharge and water level was $0.04 \text{ m}^3/\text{s}$ and 20 cm respectively. For the recalibration stage, a slot by orientation of 45 degrees to flow direction and width equal to 0.25 of pier diameter was implemented through the whole length of the pier which was extender to the sand bed. In this case, time step and roughness obtained 3s and 9.6 mm. In the

recalibration stage, local scour depth was 84 mm where the experimental results of Kummar et al. (1999) showed 83 mm. Fig. 5 illustrates the bed topography at the end of the recalibration stage for evaluating the skewed slot effect in local scouring depth.

Effect of four other slot orientations (i.e., $\theta = 0^\circ, 10^\circ, 20^\circ$ and 30°) on local scour depth was numerically simulated by SSIIM model whereas the boundary conditions were similar for all other runs and they just differ in geometric parameter of slot orientation. Fig.

6 shows horizontal flow velocity vectors and their deflection when they confront with skewed slot.

Fig. 7 illustrates the bed topography at the end of simulation procedure for each slot orientation. As it can be clearly seen from the outputs of SSIIM model in Fig. 7, due to the flow deflection after facing the oriented slot, down flow vortices and consequent horseshoe

vortex will lose its symmetric nature. Moreover, tendency of horseshoe vortex is to extend along the slot direction and gain an asymmetric pattern and so scour hole shape will be asymmetric in the same way. Furthermore, it seems that by increasing the slot skew to flow direction, horseshoe vortex and the resulting bed changes in the vicinity of bridge pier tend to further extend along the slot direction.

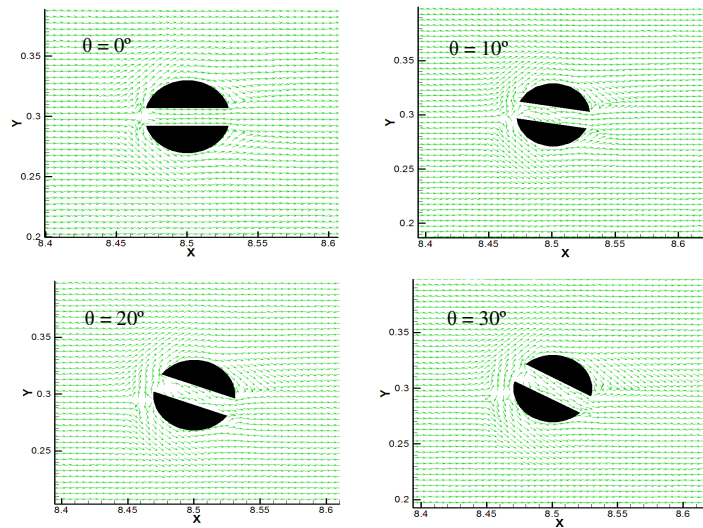


Fig. 6. Deflection of flow velocity vectors after facing skewed slots.

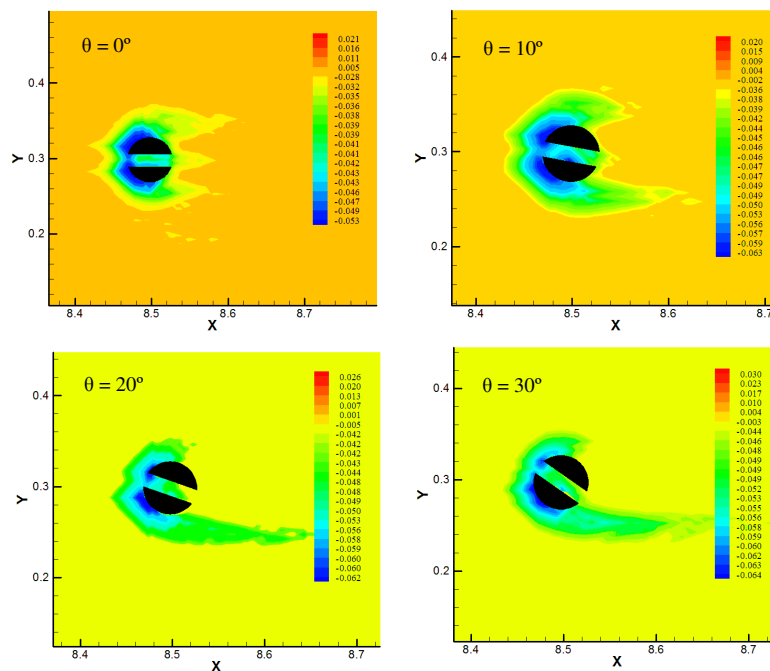


Fig. 7. Bed changes pattern in the vicinity of pier with different degrees of skewed slot

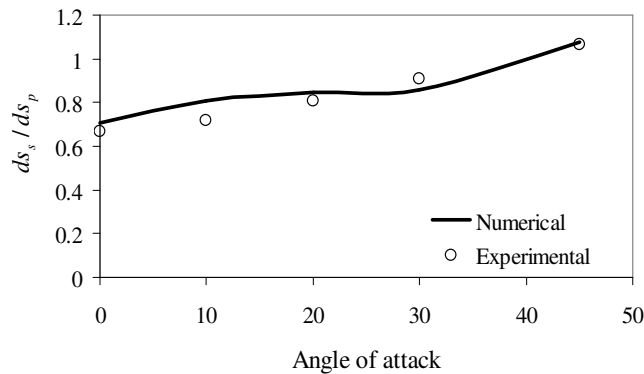


Fig. 8. Variation of local scouring depth around slotted piers with different degrees of skew

Fig. 8, demonstrates the variation of maximum local scour depth in the vicinity of circular pier versus slot skew degree that was obtained from numerical simulations by SSIIM program. The numerical results were compared to experimental data which were gained by Kummar et al. (1999) and a good agreement has been illustrated between numerical and experimental results. It must be noted that the experimental data provided by Kummar et al. (1999) were summarized in the form of a non-dimensional graph.

There is a general trend that, indicated by both in numerical and experimental results, when angle of attack to a slotted pier goes up, scour depth increases and the reduction of scour depth due to slot extension starts to offset. More specifically, when the angle of attack is about 40 degrees, the scour depth in this occasion will be the same as one of pier without slot. It seems that when angle of attack with slot starts to increase, turbulence further magnifies. In addition, downflow and horseshoe vortices will empower as a result and subsequently the reduction effect of slot on local scouring becomes neutral by the reinforced vortices.

5. Conclusion

The numerical simulation of geometric parameters effects of rectangular slot with and without orientation on local scouring

around circular pier has been conducted by employing a SSIIM model. The following results are obtained from the present study:

- When the angle of flow approach with slot is equal to zero, rectangular slot has a potential to reduce the local scouring, particularly when the slot length increases respect to the water surface. The local scour depth can be reduced up to 30% in the vicinity of a pier with a slot which was implemented through the whole length of pier and extender to the bed, compare to a pier without slot. It is due to this fact when the length of rectangular slot increases, down flow vortex as well as horseshoe vortex becomes weaker than the case in which there is not any apparatus implemented through the pier. However, additional studies on slots with different widths should be done in order to develop an applicable designing relationship.
- Although slots could reduce the local scour depth, in most of the practical cases, piers are skewed to flow and it was depicted that slots are likely to be ineffective especially when the angle of flow approach with slot increases. It is noticeable that when the slot skew to the approach flow is about 30 to 45 degrees, the local scour depth will be similar to the condition without slot and from this stage

on, by increasing the slot skew, the scour depth will exceed the original local scour depth around the pier without slot. In this condition, the turbulence is predominant and the reduction factor of slot on local scouring starts to be offset.

Nomenclature

a	reference level set equal to the roughness height (m)
C_{bed}	sediment concentration close to bed (kg/kg)
d	the sediment particle diameter (m)
D_{50}	mean size of sediment (m)
g	acceleration of gravity (m/s ²)
k_s	roughness equivalent to a diameter of particles on the bed (m)
$q_{s,1}$	suspended-load sediment transport in x direction
$q_{s,2}$	suspended-load sediment transport in y direction
q_{tx}	bed-load sediment transport in x direction
q_{ty}	bed-load sediment transport in y direction
Sc	Schmidt number
u_i	flow velocity in i direction (m/s)
u_x	shear velocity (m/s)
w	fall velocity of sediment (m/s)
y	distance to the wall (m)
z_b	bed elevation (m)
α_b	direction of bed-load sediment transport
σ_g	geometric standard deviation of sediment size distribution
ρ_w	density of water (kg/m ³)
ρ_s	density of sediment (kg/m ³)
λ	the porosity of bed material
ν_T	eddy viscosity (Pa.s)
Γ_T	diffusion coefficient
τ	the bed shear stress (Pa)
τ_c	the critical bed shear stress (Pa)
ν	viscosity of the water (Pa.s)

κ constant equal to 4.0

References

- Chabert J., and Engeldinger P., (1956). Etude des affouillements autour des piles de ponts. Laboratoire National d'hydraulique.
- Chew Y. M., (1992). Scour protection at bridge piers. *Journal of Hydraulic Engineering ASCE*, 1260-1269.
- Dehghani A. A., Esmaeili T., Kharaghani S. and Pirestani M. R., (2009). Numerical simulation of scour depth evolution around bridge piers under unsteady flow condition. *Water Engineering for a Sustainable Environment*. Vancouver: IAHR, 5888-5895.
- Esmaeili T., (2009). *Hydraulic and Geometric Numerical Simulation of Scouring around Concrete Bridge Piers (Case Study)*. M.Sc. Thesis, Tehran: Islamic Azad University-South Tehran Branch.
- Esmaeili, T., Dehghani, A.A., Zahiri A. R. and Suzuki K., (2009). 3D Numerical Simulation of Scouring Around Bridge Piers (Case Study: Bridge 524 crosses the Tanana River). *International Conference on Civil Engineering and Environment*. Venice: World Academy of Science, Engineering & Technology, 1557-1561.
- Ettema R., (1980) *Scour at bridge piers*. Rep. No. 112, Auckland: University of Auckland.
- Garg V., Setia B. and Verma D.V.S., (2008). Prevention of scour by combination of scour protection devices around bridge piers. *River flow 08*. Izmir: Altinakar, Kokpinar, Gogus, Tayfur, Kumcu & Yildirim (eds), 1637-1643.
- Grimaldi C., Gaudio R., Calomino F. and Cardoso A.H., (2009). Countermeasures against Local Scouring at Bridge Piers: Slot and Combined System of Slot and Bed Sil. *Journal of Hydraulic Engineering, ASCE*, 425-432.

- Gupta A. K. and Gangadharaiiah T., (1992). Local scour reduction by a delta wing-like passive device. *Proceeding of 8th Congress of Asia & Pacific Reg. Div.2 (CWPRS)*. Pune: APD-IAHR.
- Kumar V., Ranga Raju K. G., and Vittal N., (1999). Reduction of local scour around bridge piers using slots and collars. *Journal of Hydraulic Engineering*, ASCE 1302-1305.
- Mendoza Cabrales C., (1993). Computation of flow past a pier mounted on a flat plate. *Proceeding of ASCE Water Resources Engineering*. San Francisco, California: ASCE, 899-904.
- Mia F. and Nago H., (2003). Design Method of Time-Dependent Local Scour at Circular Bridge Pier." *Journal of Hydraulic Engineering*, 420-427.
- Moncada M. A.T., Aguirre-Pe J., Bolivar J. C. and Flores E. J., (2009). Scour protection of circular bridge piers with collars and slots. *Journal of Hydraulic Research*, 119-126.
- Murillo J. A., (1987). The scourge scour. *Journal of Hydraulic Engineering ASCE*, 66-69.
- Odgaard, A. J. and Wang Y., (1987). Scour prevention at bridge piers. *Proceeding of Hydraulic Engineering National Conference*. Ragan, Virginia: ASCE, 523-527.
- Olsen, N. R. B, Jimenes O. F., Abrahamsen L. and Lovoll A., (1999). 3D CFD modeling of water and sediment flow in a hydropower reservoir. *International Journal of Sediment Research*, 1-8.
- Olsen N. R. B., (2008). *Norwegian University of Science and Technology*. 2007. <http://www.ntnu.no> (accessed 04 14).
- A three dimensional numerical model for simulation of sediment movement in water intakes with multiblock option. *Norwegian University of Science and Technology*. 2007. <http://www.ntnu.no> (accessed 04 15, 2008).
- Roheds J. and Trent R. E., (1993). Economic of floods, scour and bridge failures. *Stream stability and scour at highway bridges*. Reston, Virginia: ASCE, 928-933.
- Tafarojnoruz A., Gaudio R. and Dey S., (2010). Flow altering countermeasures against scour at bridge piers: a review. *Journal of Hydraulic Research*, 441-452.
- Tanaka S. and Yano M., (1967). Local scour around a circular cylinder. *Proceeding of 12th IAHR Congress*. Fort Collins, Colorado The Netherlands: IAHR, 193-201.
- Thomas Z., (1967). Local scour around a circular cylinder. *Proceeding of 12th IAHR Conference*. Fort Collins, Colorado: IAHR, 125-134.